CERN – EUROPEAN ORGANIZATION FOR NUCLEAR RESEARCH

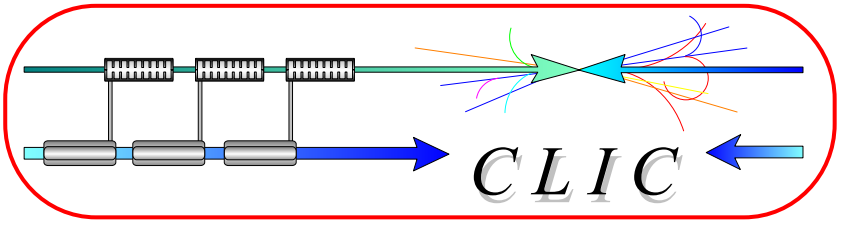

CLIC-Note-664

FAST SWITCHING DEVICES AND INDUCTION RF AT CLIC

R. Assmann, H. Braun, F. Caspers, R. Corsini, D. Schulte, F. Zimmermann
CERN, Geneva, Switzerland

P.N. Burrows
Oxford University, United Kingdom

CERN-OPEN-2006-031
28 / 07 / 2006

Abstract

We survey possible applications of fast switching devices and induction rf at the Compact Linear Collider (CLIC). These applications include extraction kickers for the combiner rings, modulators for the drive-beam linac, fast intra-train feedback, induction crab cavities, halo kickers, emergency kickers, long-range beam-beam compensation, damping-ring barrier rf, pulsed linac wigglers, positron capture, and spent-beam handling.

Presented at :RPIA2006, Recent Progress in Induction Accelerators, KEK, Tsukuba, Japan, March 7-10, 2006

Geneva, Switzerland
28th July 2006

Fast Switching Devices and Induction RF at CLIC

R. Assmann, H. Braun, F. Caspers, R. Corsini, D. Schulte, F. Zimmermann, CERN, Geneva, Switzerland;
P.N. Burrows, Oxford University, United Kingdom

Abstract

We survey possible applications of fast switching devices and induction rf at the Compact Linear Collider (CLIC). These applications include extraction kickers for the combiner rings, modulators for the drive-beam linac, fast intra-train feedback, induction crab cavities, halo kickers, emergency kickers, long-range beam-beam compensation, damping-ring barrier rf, pulsed linac wigglers, positron capture, and spent-beam handling.

OUTLINE

This report is organized as follows. We first present a brief overview of the CLIC project. We then describe two systems which are absolutely required for the baseline CLIC design and for which the RPIA (Recent Progress in Induction Acceleration) 2006 workshop may provide cost-effective solutions, namely (1) the extraction kicker for the first drive-beam combiner ring, and (2) the modulators for the drive-beam linac. In the following we address two other indispensable components for which practical conventional solutions already exist, but where alternative approaches could be interesting: the fast feedback at the collision point, and crab cavities. Lastly, we walk through a list of new ideas, which are not essential, but which could further boost the CLIC performance. These include the use of induction rf in the damping ring, emergency beam dumps along the main linac, halo kickers, long-range beam-beam compensation, pulsed flux concentrator for positron capture after the target, pulsed wigglers in the linac, and pulsed fields for the extraction of the spent beam.

COMPACT LINEAR COLLIDER – CLIC

CLIC will be an electron-positron collider with a centre-of-mass energy reach of 3–5 TeV. Its physics programme is fully complementary to that of the Large Hadron Collider (LHC), which is on track to start operation in 2007. The physics motivation for CLIC is to probe beyond the standard model and to understand the origin of mass, the unification of forces and the origin of flavors.

Key features of CLIC are (1) a high accelerating gradient of about 150 MV/m which implies a high rf frequency and a ‘compact’ size; (2) two-beam acceleration, where the energy is stored in a drive beam, and the rf power is generated locally, as illustrated in Fig. 2; (3) a central injector, comprising a fully loaded normal-conducting linac with 96% rf-to-beam power-transfer efficiency and involving ‘rf frequency multiplication’ and ‘power compression’.

A concise history of CLIC as well as its near-term future are shown in Fig. 1. From 1995 onwards, the CLIC Test Facility no. 2 (CTF-2) demonstrated the feasibility of two-beam acceleration. In 2003 the CLIC physics report was published [1]. One year later, the CLIC R&D schedule was accelerated, in order to obtain answers to all ILC-TRC feasibility questions by 2009 [2]. It is foreseen to produce a preliminary cost estimate in 2008. From Fig. 1 it can be inferred that CLIC is about 5 years behind the International Linear Collider. The feasibility of CLIC will be demonstrated about 1 or 2 years after the start of LHC operation, which is the right time for a decision on a major new facility.

Two-beam acceleration was originally proposed by A. Sessler [4] in 1982, and for CLIC by W. Schnell [5] in 1986. Figure 2 shows a schematic of the CLIC drive and main beams running in parallel. The intense low-energy drive beam is decelerated and its energy converted into rf power, which is transferred to the accelerating rf structures of the higher-energy, low-emittance and lower-charge main beam.

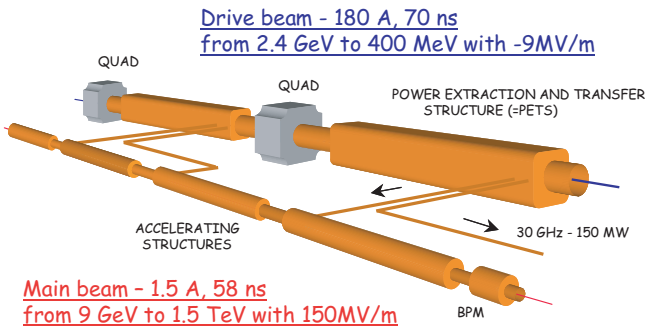

Figure 2: Schematic of CLIC two-beam acceleration module; 6000 such modules are needed for a 3-TeV collider.

The primary goal of the CLIC scheme is achieving a high accelerating gradient of 150 MV/m or above. In 2002, at the previous facility CTF-2, high gradient tests of structures with molybdenum irises reached 190 MV/m peak accelerating gradient without any damage [6], well above the nominal CLIC accelerating field. These results, which constitute a world record, are displayed in Fig. 3. Since 2005, at the 3rd generation test facility CTF-3, 30-GHz rf pulses of the nominal 70-ns lengths are being produced for struc-

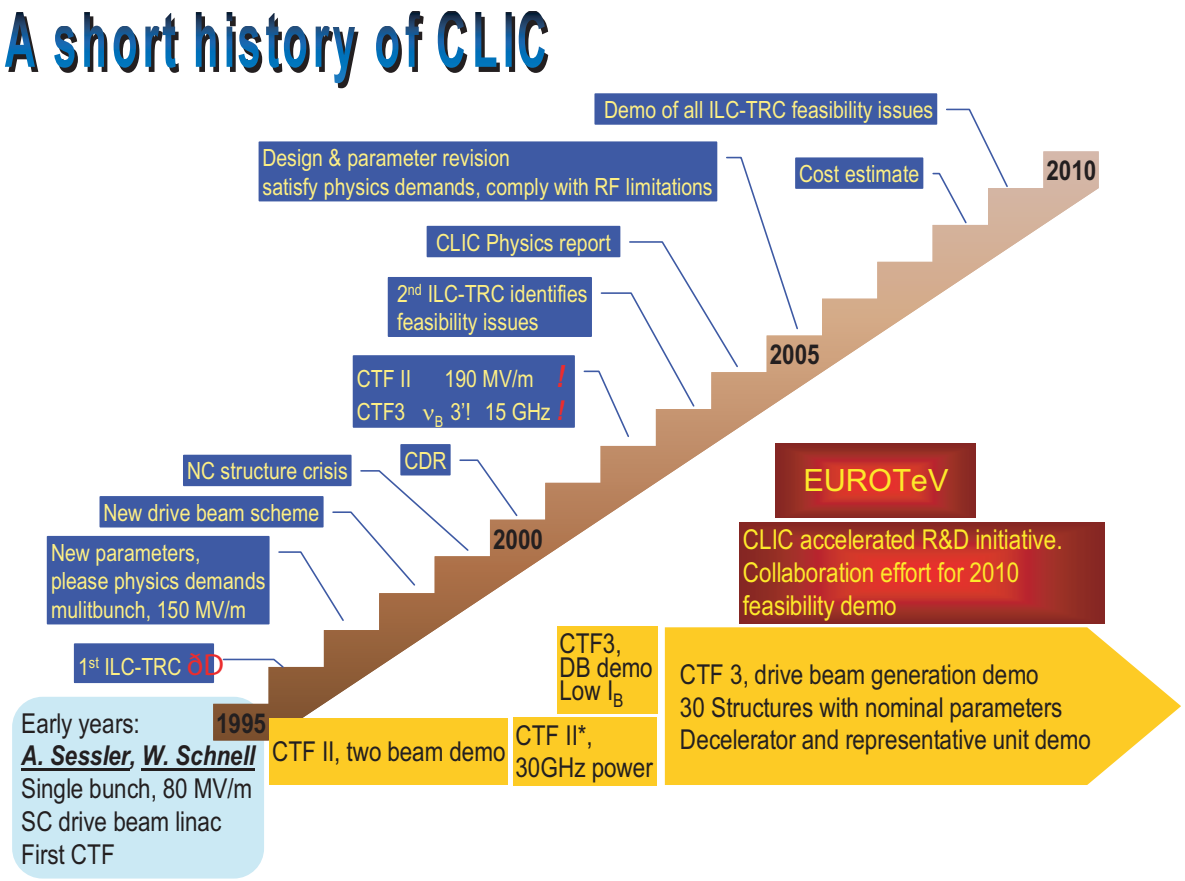

Figure 1: A short history of CLIC [3].

ture tests with the design CLIC gradient. This is an important milestone on the path towards demonstrating CLIC feasibility.

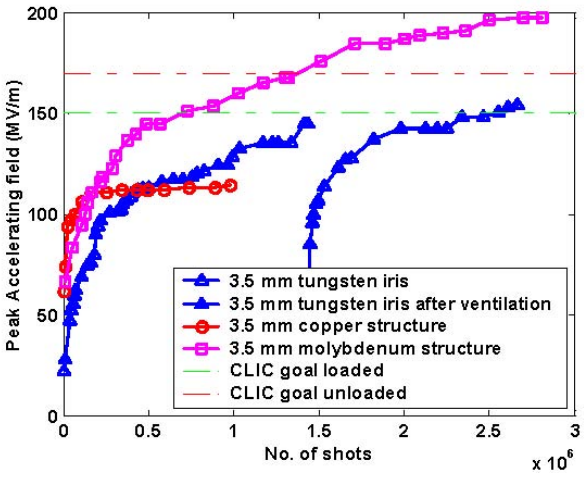

Figure 3: Conditioning history of three copper accelerating structures with either copper, molybdenum or tungsten irises at CTF-2 [6].

Recently, the design and production of the rf structures were modified and optimized [7]. The CLIC main-linac rf structures are now assembled from 4 quadrants, without any brazing or welds in the direction orthogonal to the beam image-current flow. The photo of a new structure is displayed in Fig. 4.

Advantages of the CLIC scheme, in addition to the high gradient and short length of the linac, are that it can easily be built in stages, raising the energy simply by the gradual addition of main-linac modules, like those shown in Figure 2, and that its tunnel does not house any active elements. An artist's view of the CLIC tunnel cross section is displayed in Figure 5. The tunnel provides space for two beam pipes, quadrupole magnets, plus the rf & transfer structures, but, e.g., for neither klystrons nor modulators. At CLIC, klystrons and modulators are indeed rather few in total. Their number is comparable to those in use at the SLAC linac. They are concentrated in the CLIC central injector complex.

Table 1 lists the main parameters of CLIC at 3 TeV. The overall performance is characterized by centre-of-mass energy, luminosity, rf gradient (site length), total AC power, and transfer efficiency from wall-plug power to main-beam power.

Figure 6 present a bird's eye view of the entire CLIC complex for the 3-TeV collider. Figure 7 indicates the lo-

Table 1: CLIC Parameters at 3 TeV

centre-of-mass energy	$E_{\rm cm}$	3000	GeV
main linac rf frequency	$f_{\rm rf}$	30	GHz
luminosity	L	6.5	10^{34} cm^{-2}s^{-1}
luminosity (in 1% of energy)	$L_{99\%}$	3.3	10^{34} cm^{-2}s^{-1}
linac repetition rate	$f_{\rm rep}$	150	Hz
particles per bunch	N_b	2.56	10^9
bunches per train	n_b	220	—
bunch separation	$\Delta t_{\rm sep}$	0.267	ns
bunch train length	$\tau_{\rm train}$	58.4	ns
beam power / beam	P_b	20.4	MW
unloaded / loaded gradient	$G_{\rm unl,l}$	172, 150	MV/m
overall two-linac length	$l_{\rm linac}$	28	km
total beam delivery length	$l_{\rm BDS}$	2×2.6	km
proposed site length	$l_{\rm tot}$	33.2	km
totao ac site power	$P_{\rm tot}$	418	MW
wall plug (rf) to main-beam power efficiency	η	12.5	%

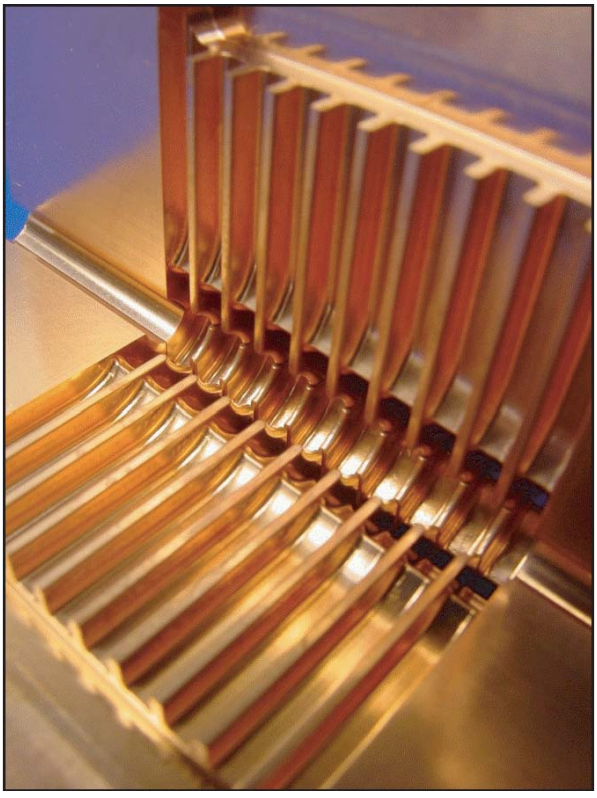

Figure 4: CLIC hybrid-damped accelerating structure [7] with damping waveguides and slotted irises, optimized geometry, assembly without brazing, and molybdenum iris tips [8].

cations of various possible components based on 'RPIA' technology, which are discussed later in this report. As can be seen in this figure, modern pulsed power technologies and new materials could find numerous interesting applications throughout the CLIC complex.

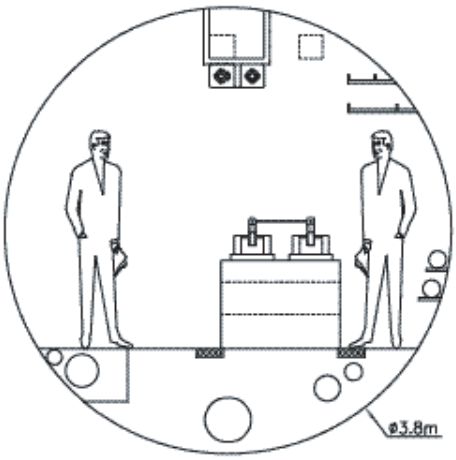

Figure 5: Schematic of the CLIC tunnel cross section. The tunnel is simple, with a diameter of 3.8 m, and no active elements.

The CLIC rf power source can be thought of as a "black box" combining very long rf pulses, and transforming them into many short pulses with higher power at and higher frequency, as is illustrated in Fig. 8.

The actual 'building blocks' of this rf power source — a fully loaded traveling-wave linac for drive-beam acceleration, and transverse rf deflectors for beam combination and separation — are illustrated in Figs. 9 and 10. The overall layout of the CLIC rf power source, i.e., the drive-beam complex, is displayed in Fig. 11, where we again indicate locations of some elements conceivably based on 'RPIA' technologies, namely the modulators of the drive-beam linac, and the extraction kickers in the two combiner rings.

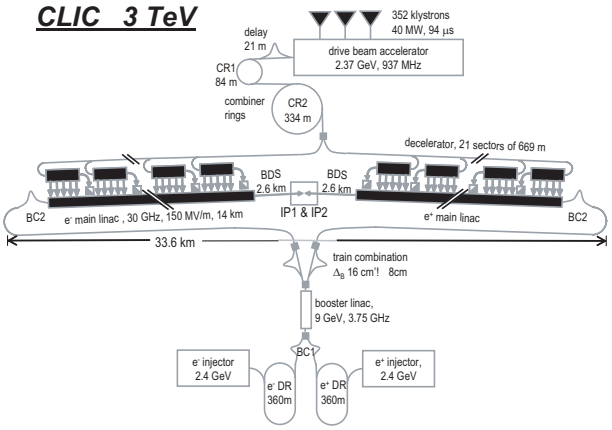

Figure 6: Overall layout of CLIC at 3 TeV [Courtesy H. Braun].

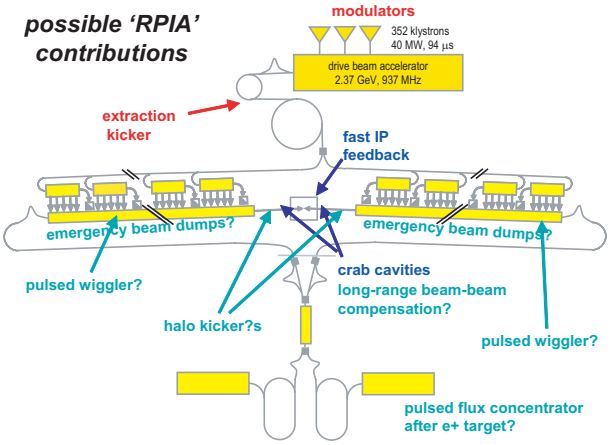

Figure 7: Overall layout of CLIC at 3 TeV, highlighting possible 'RPIA' contributions.

After being accelerated highly efficiently, with full beam loading, in a traveling-wave linac, the time structure of the beam is fundamentally modified by passing through a delay line (half of the beam) and two combiner rings. The net result is 21 bunch trains with 32 less spacing between bunchers and correspondingly higher current. This transformation is graphically sketched in Fig. 12. The final trains represent a unique power source in the 10s of GHz frequency range, and they are used to drive sections of the main high-gradient linac, which accelerates the two colliding electron and positron beams.

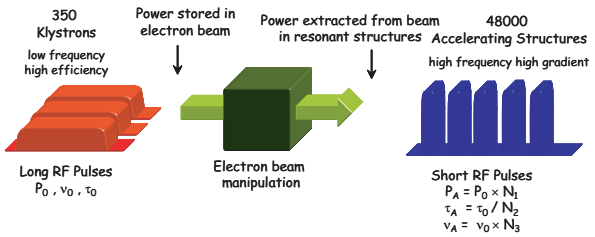

Figure 8: Schematic view of the CLIC rf power source as 'black box' [Roberto Corsini, HEP2005] [9].

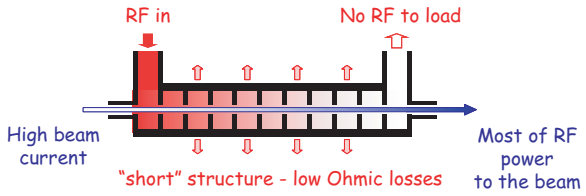

Figure 9: Acceleration with full beam loading in the traveling-wave rf structures of the drive beam linac [Roberto Corsini, HEP2005] [9].

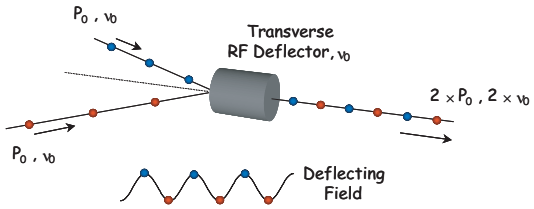

Figure 10: Beam combination and separation by transverse rf deflectors [Roberto Corsini, HEP2005] [9].

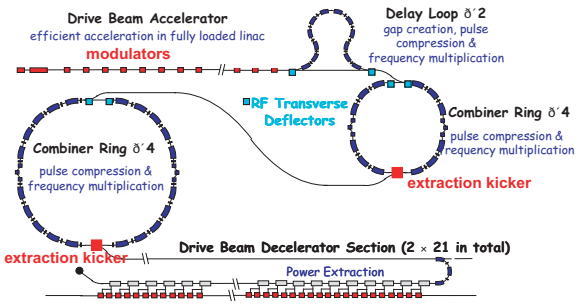

Figure 11: Overall layout of CLIC rf power source, including locations of transverse rf deflectors (in blue) and possible RPIA elements (in red) [Roberto Corsini, HEP2005] [9].

ESSENTIAL SYSTEMS

Drive-Beam Modulators

The modulators of the drive-beam linac should provide 40 MW rf power in a 100-μs pulse, with an energy per pulse of about 4 kJ, at 150 Hz. This type of modulator will be used to feed a 937-MHz multi-beam klystron and to generate a long rf pulse.

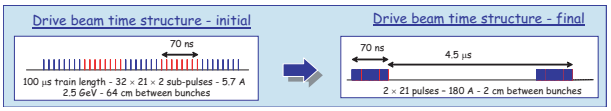

Figure 12: Initial and final CLIC drive beam time structure [Roberto Corsini, HEP2005] [9].

The average power demanded from the modulator is more than three times higher than for some other projects:

- The main linac modulators of TESLA/ILC provide 10 MW with 1.7-ms pulse length for a 1.3 GHz rf system, with an energy per pulse of 20 kJ at 5 or 10 Hz [10].
- The modulators of the FNAL s.c. proton driver should provide 20 MW with a pulse length of about 1 ms, for a 1.2 GHz rf system, at 2.5 or 10 Hz [11].
- A prototype solid-state induction modulator for the demised NLC/JLC/GLC project (1-beam klystron), provided 640 MW, with 1680 A current at 380 kV voltage, over 3 μs pulse length, which amounts to about 2 kJ per pulse, for a 11.4 GHz rf system, at 120 Hz [12].

Figure 13 illustrates the CLIC drive-beam linac rf power source with two long-pulse modulators, each feeding a multi-beam klystron. The main parameters of the modulators are summarized in Table 2.

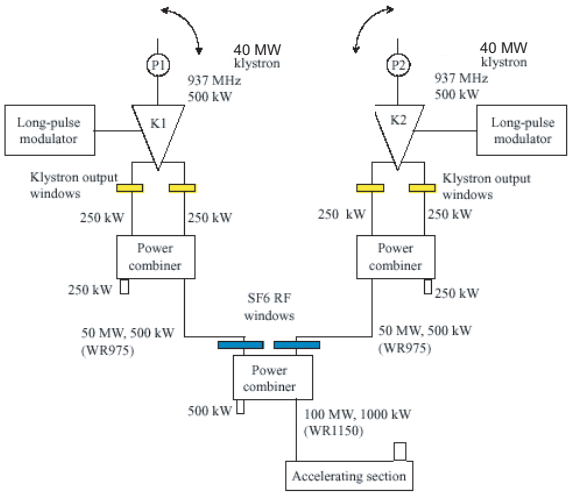

Figure 13: The 40-MW multibeam klystron rf network module [13].

Combiner-Ring Extraction Kicker

The extraction kicker in the first combiner ring is the most challenging. Figure 14 sketches the time structure of the required kicker pulse. A rise time of less than 70 ns is followed by a flat top of 210 ns to extract the combined bunch train. Next come a fall time of again less than 70 ns, and then a zero kick over 770 ns, during which time the next combination is accomplished. This pattern is repeated 83 times, giving a pulse length of about 100 μs. The pulse repetition frequency is 150 Hz.

Table 2: Parameters of CLIC drive-beam modulator.

peak power	40 MW
pulse length	100 ms
pulses / second	150

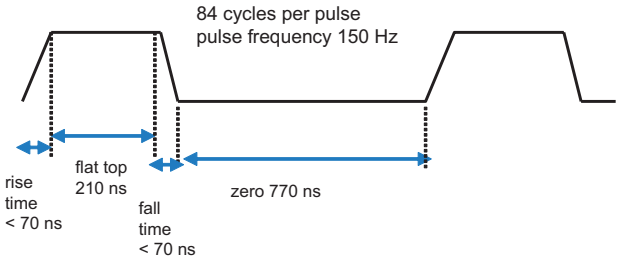

Figure 14: Time structure of combiner-ring extraction-kicker pulse.

The combiner ring operates at a beam energy of 2 GeV. For estimating the kicker strength needed, we assume a beta function at the extraction point of order 10 m and a minimum required deflection angle of 10 mrad. The main parameters of the extraction kicker are summarized in Table 3.

Table 3: Parameters of extraction kicker for 1st combiner ring.

kick strength	$>$0.1 Tm or $>$20 MV
rise time	$<$ 70 ns
flat top	210 ns
pulse period	1120 ns
cycles / pulse	84
pulses / second	150

INDISPENSABLE SYSTEMS FOR WHICH CONVENTIONAL SOLUTIONS EXIST

Fast Intra-Train IP Feedback

The fast intra-train feedback at the interaction point (IP) is the 'last line of defense' against relative misalignments of the two colliding beams [14]. The key component of such feedback are beam-position monitors (BPMs), signal processor, fast driver amplifier, electromagnetic kicker, and

a fast feedback circuit. Two schematics of the IP feedback are shown in Figs. 15 and 16 at various levels of abstraction. The feedback circuit contains a delay loop for preventing 'under-correction' after one turn-around time.

The best prototype to date is FONT3 which was designed and constructed by a group from Queen Mary U. and Oxford University in the UK, and tested with beam at the KEK-ATF test facility [14, 15]. As detailed further below, the beam experiments with the ultrafast FONT3 have demonstrated a latency as low as 23 ns, about a third of the CLIC pulse length, and only a little short from the FONT3 design goal of 20 ns.

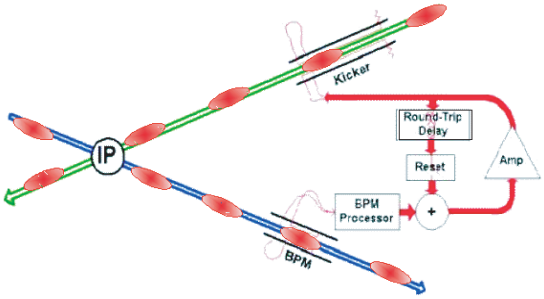

Figure 15: Schematic of intra-train feedback for interaction point with crossing angle; the deflection of the outgoing beam is recorded by a BPM and a correcting kick is applied to the incoming other beam [15].

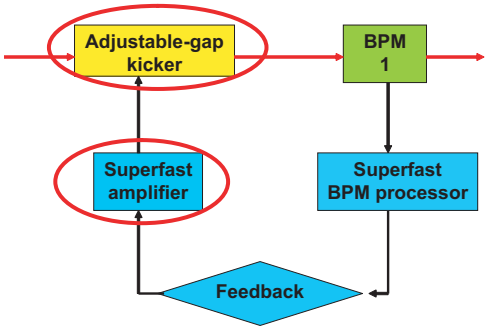

Figure 16: Schematic circuit of IP-feedback key components [14].

Kicker driver amplifiers developed for the FONT1 (at NLCTA [16]) and FONT3 IP feedback systems are displayed in Figs. 17, 18 and 19. FONT1 used a 3-kW tube amplifier, its successor FONT2 a solid-state amplifier, and FONT3 an ultrafast solid-state amplifier. The most compact FONT3 system provides the drive power which would be needed for the International Linear Collider (ILC). FONT1, FONT2 and FONT3 employed analogue signal processing, as required for CLIC, while the ILC beam parameters demand further developments and tests of a digital system.

Figure 17: Components of FONT1 3-stage tube amplifier [14].

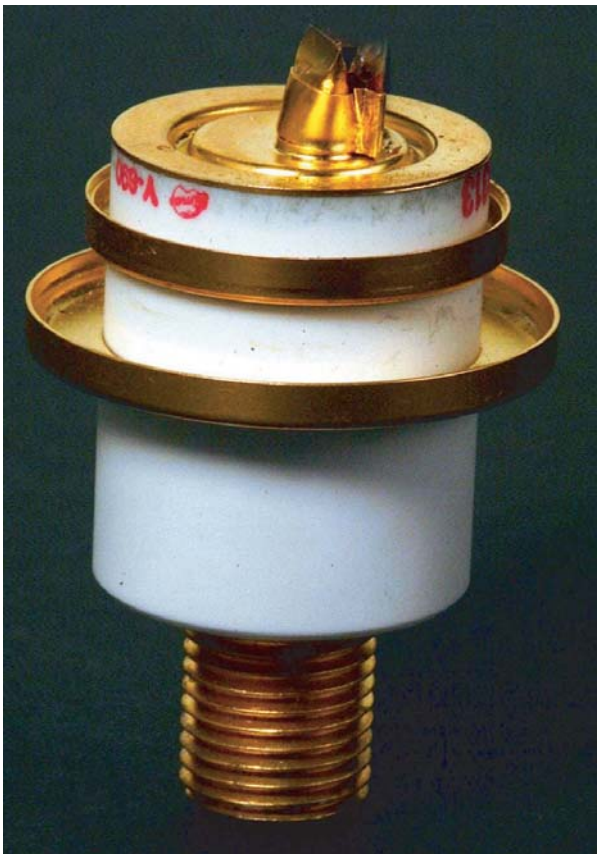

Figure 18: Components of FONT1 3-stage tube amplifier [14].

The installation of the FONT3 BPMs and amplifier-feedback systems at the KEK/ATF beamline is illustrated by the photos in Figs. 20 and 21.

The FONT3 latency budget is detailed in Table 4. A total latency of 20 ns was expected. The experimental result, reproduced in Fig. 22, showed a slightly larger value of 23

Figure 19: FONT3 printed-circuit-board amplifier and feedback [14].

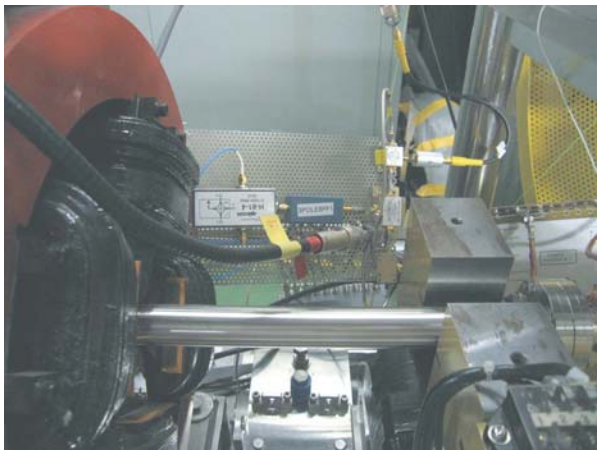

Figure 20: FONT3 BPM processor board in the KEK-ATF beam line [14].

ns.

Table 4: FONT3 latency budget

time of flight kicker - BPM	4 ns
signal return time BPM - kicker	6 ns
→ **irreducible latency**	**10 ns**
BPM processor	5 ns
amplifier & feedback	5 ns
→ **electronics latency**	**10 ns**
⇒ **total latency budget**	**20 ns**

The CLIC IP feedback requirements are as follows. The CLIC train length is about 63 ns, and, hence, very similar to that of the ATF. The time of flight from the kicker to the IP is about 7 ns assuming a 2 m distance. The feedback should have a range of 50 rms vertical beam sizes, or about 50 nm. This translates into a maximum integrated deflecting

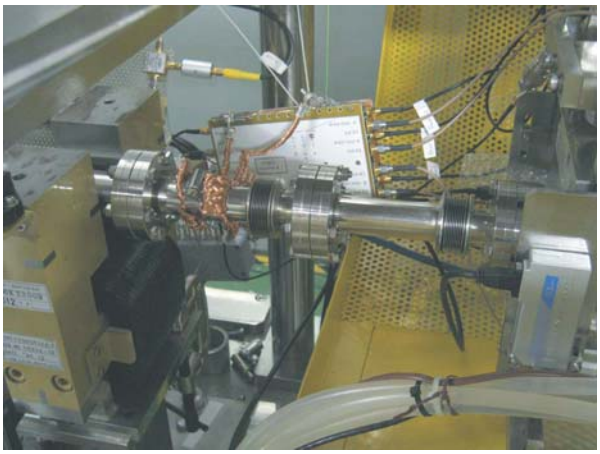

Figure 21: FONT3 amplifier-feedback board in the KEK-ATF beam line [14].

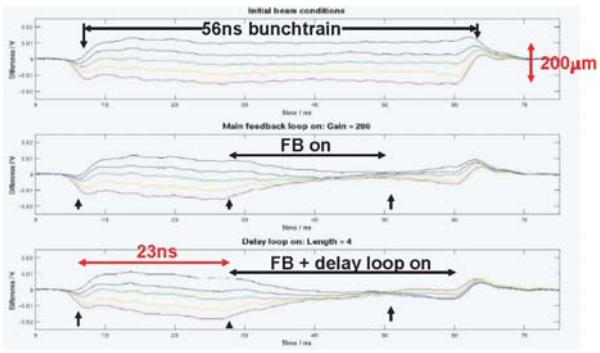

Figure 22: Experimental measurement of FONT3 latency at KEK-ATF on 3 June 2005. Each curve represents the beam position as a function of time during a bunch train passage. The different traces correspond to different initial conditions. The top graph was recorded without feedback; for the center picture the main feedback loop is active; in the bottom picture also the delay loop was turned on [14].

magnetic field, Bl, of 60 μTm, or an equivalent electric field of 19 kV. For example, considering a stripline kicker, we may estimate the corresponding stripline current as

$$I_{\rm sl} \approx \frac{\pi (Bl) d}{L \mu_0} \approx 31\,{\rm A}\ , \qquad (1)$$

where $L \approx 20$ cm is the stripline length and $d \approx 2$ cm the assumed distance between stripline and beam. With a resistance of 5Ω the peak power needed is about 5 kW. Requirements for the CLIC IP feedback are compiled in Table 5.

Crab Cavities

The CLIC design foresees a crossing angle of 20 mrad at the interaction point. This crossing angle is necessary to remove the spent beam including coherent pairs and beam-

Table 5: Parameters of CLIC intra-train IP feedback.

voltage	>19 kV
current	31 A
response time	few ns
bunches / pulse	220
pulses / second	150

strahlung photons, and to avoid the multibunch kink instability [17, 18]. On the other hand, if no measures are taken, the luminosity decreases with crossing angle by the geometric reduction factor

$$R_\theta = \frac{1}{\sqrt{1+\Theta^2}} , \qquad (2)$$

where

$$\Theta = \frac{\theta_c \sigma_z}{2\sigma_x} \qquad (3)$$

denotes the Piwinsi angle. Inserting typical CLIC parameters, $\sigma_x \approx 60$ nm, $\sigma_z \approx 31$ μm, $\theta_c \approx 20$ mrad, we have $\Theta \approx 5.2$ and $R_\theta \approx 0.19$. Therefore, CLIC would achieve only 19% of the ideal head-on luminosity.

Crab cavities which effectively restore the head-on luminosity of a linear collider [19] therefore are indispensable for CLIC. The principle of the 'crab crossing' is shown in Fig. 23. The crabbing is realized with transverse dipole-mode rf cavities. The crab cavity rf deflects the head and tail of the bunch in opposite direction.

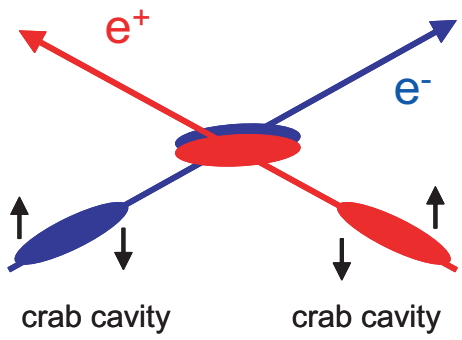

Figure 23: Schematic of the crab-crossing principle; head and tail of the bunch receive a deflection in opposite direction, so that the collision effectively becomes head-on.

With a bunch spacing of 0.267 ns, the crab rf frequency must be a multiple of 3.75 GHz. The R_{12} matrix element from the crab-cavity location to the IP is of order 10 m. The crab voltage required is

$$V_{\rm crab} = \frac{cE_0 \tan(\theta_c/2)}{e2\pi f_{\rm rf} R_{12}} \approx \frac{cE_0}{e4\pi f_{\rm rf} R_{12}} \theta_c , \qquad (4)$$

which amounts to 20 MV at 3.75 GHz or 1 MV at 30 GHz.

There exists a tight tolerance on relative phase jitter between the crab cavities on the left and right side of the IP. Such relative phase jitter would steer the beam out of collision. The phase tolerance is

$$\Delta\phi_{\rm crab} = \frac{\Delta x_{\rm max} 4\pi}{\lambda_{\rm rf}\theta_c} , \qquad (5)$$

where $\Delta x_{\rm max}$ is the maximum permissible offset between the two beams. Taking as maximum allowed offset 20% of the rms IP beam size (about 12 nm), the phase tolerance is 94 μrad at 3.75 GHz or equal to 4 fs independent of frequency.

Timing tolerances for crab cavities at various projects are compared in Table 6. The only crab cavities under construction so far are those for KEKB, which is a storage-ring B factory and for which the timing tolerance has a fairly loose value of 6 ps. The tolerances for crab cavities at the ILC would be 200 times tighter and those for CLIC yet another factor of 8 more demanding. It is interesting to note that a phase stabilization system meeting a 0.02-ps jitter tolerance is presently under development for the X-ray FEL at DESY [20].

Table 6: Left-right timing tolerance for crab cavities of various projects, computed for a beam-beam offset at the collision point of less than $0.2\sigma_x^*$.

	KEKB	Super-KEKB	ILC	CLIC
σ_x^*	100 μm	70 μm	0.24 μm	0.06 μm
θ_c	$\pm$11 mrad	$\pm$15 mrad	$\pm$5 mrad	$\pm$10 mrad
Δt	6 ps	3 ps	0.03 ps	0.004 ps

Could we employ an induction rf system to achieve the crab crossing? Figure 24 compares the conventional crabbing scheme, where bunches are placed at the zero crossing of a harmonic rf wave, with two alternative induction-rf crabbing scheme, using either a linear increase in the transverse crab voltage along the full bunch train or a repetitive sawtooth pattern.

The bunches in CLIC are spaced at 8 cm (0.267 ns). Therefore, the minimum frequency of a classical harmonic crab cavity is 3.75 GHz, a situation which is sketched in the top picture of Fig. 24. The linear slope across the bunch near the zero crossing of the rf wave is used for crabbing.

With induction rf we could generate a long linearly rising voltage slope, as indicated in the center picture. Unfortunately, the value of the required slope is prohibitively high, namely 4.7×19^{17} V/s, corresponding to a voltage increase of 28 GV over the linac pulse length of 60 ns, which appears beyond the present state-of-the-art in induction rf. In addition, with this type of crabbing different bunch pairs would not collide at the same horizontal position, but, along a bunch train, the collision point would shift horizontally by $\Delta x^*_{\rm train} \approx 19$ cm, which is large compared with the size of the innermost particle-physics detector.

Therefore, another application of induction rf could be considered, which mimics the shape of the harmonic rf by

a sawtooth pulse. This second solution is shown in the bottom picture of Fig. 24. The voltage swing is ± 31 MV with a period of 3.75 GHz. Again, the combination of high frequency and tens of Megavolts amplitude looks rather demanding for an induction rf system with the technology at hand. Meeting the timing tolerance with induction rf might also be a challenge. Table 7 summarizes the requirements on a (induction-rf) sawtooth crabbing system at CLIC.

A cost estimate for a generic induction rf system was presented at the RPIA 2006 workshop. It amounts to 100 million US$ for 10 MV of induction rf (i.e., induction rf has the same price per unit length as normal rf, and the same price per Volt as the ILC s.c. rf) [21]. Clearly the price for a CLIC induction-crab system would not be negligible. However, it was also pointed out that the costs per Volt of the three FNAL systems have differed by more than an order of magnitude.

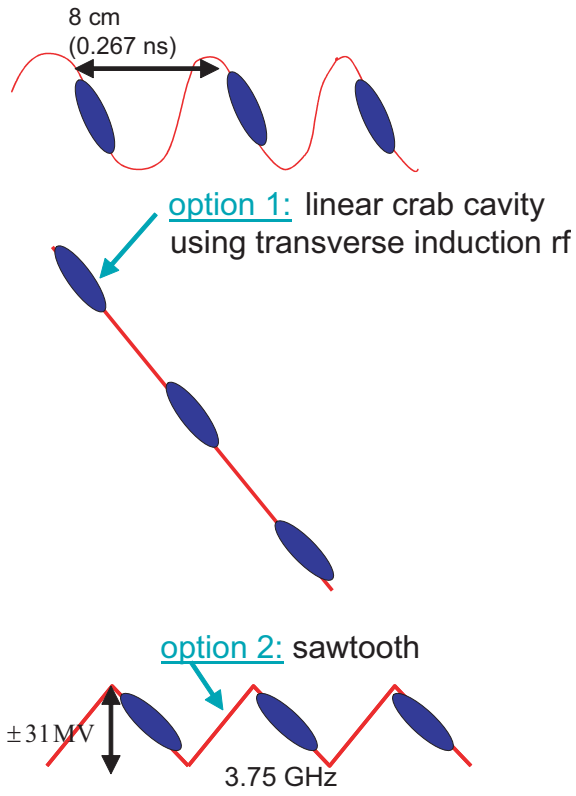

Figure 24: Comparison of conventional harmonic crab voltage (top), with two alternative schemes based on induction rf, namely linear voltage slope (center), and sawtooth (bottom).

NEW IDEAS WHICH COULD FURTHER BOOST CLIC PERFORMANCE

Induction RF in Damping Ring

The nominal CLIC damping ring produces a short Gaussian bunch ($\sigma_z \approx 1.3$ mm) in a single-harmonic rf system.

Table 7: Parameters for a hypothetical CLIC induction-rf crabbing system.

peak voltage	>30 MV
frequency	3.75 GHz
timing jitter	< 0.004 ps
cycles / pulse	220
pulses / second	150

Iterative analytical calculations [22, 23] predict a large effect of intrabeam scattering (IBS), which, e.g., increases the normalized horizontal emittance from 134 nm without IBS to 550 nm when IBS is taken into account [24].

Induction rf would allows us to flatten the bunch profile, e.g., by generating barrier buckets and creating a rectangular bunch. For a rectangular bunch of length $l_{\rm flat}$, the IBS rate would decrease, provided the bunch is long enough, namely [25]

$$l_{\rm flat} > 2\sqrt{\pi}\sigma_z \approx 5.3 \text{ mm} . \qquad (6)$$

Unluckily, an additional design constraint for CLIC is that the longitudinal rms emittance in the damping ring should not increase. Taking this as well into account, the maximum static gain in IBS growth rate due to the restricted bunch flattening turns out to be only about 10%. A variant of the above scheme would be the dynamic bunch compression with induction rf just prior to extraction, in which case all emittances need to be calculated dynamically. The beam dynamics in an induction-rf damping ring has not yet been studied in any detail, however.

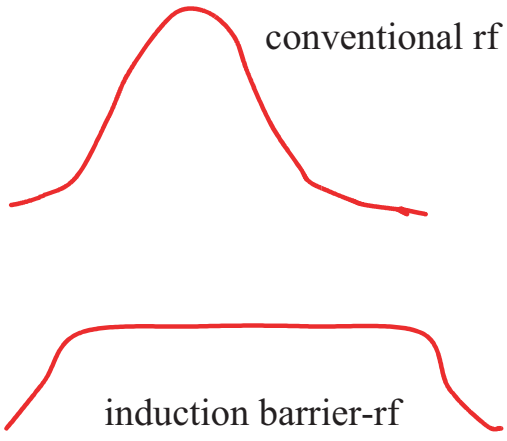

Figure 25: Artist's view of damping-ring bunch profile with harmonic rf (top) and barrier-bucket induction rf (bottom).

Table 8 lists parameters for an induction-rf system at the CLIC damping ring. The bunch frequency is half the linac frequency, but with 1.9 GHz still high. Indeed, worldwide the only storage ring operating with a higher (conventional) rf frequency, namely 2.856 GHz, is the MIT Bates South Hall Ring [26].

Table 8: Parameters for a hypothetical damping-ring induction-rf system.

voltage	>30 MV
frequency	1.9 GHz
pulses / second	cw operation

Emergency Kickers Along Main Linac

Presently the CLIC design allocates a length of 2 km per beam to collimation. The main reason for this substantial length is that the beam sizes need to be blown up, at least for the off-momentum collimator, so as to guarantee collimator survival in case of beam impact due to an upstream failure [27] (see Fig. 26). Mis-phased or unstable drive beams are likely failure modes in CLIC [29].

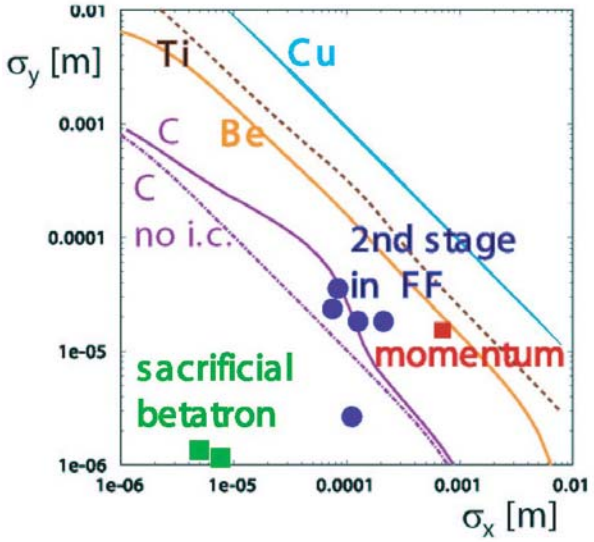

Figure 26: CLIC damage threshold diagram: minimum horizontal and vertical rms spot sizes in case of beam impact on various materials (for carbon calculations with and without the effect of image currents are shown) [27]. The nominal beam sizes at various collimator positions in the present CLIC collimation system and final focus are also indicated by the plotting symbols [28].

If the only function of the collimation system were removing the beam tails and improving the physics-detector background, it could be substantially shortened. A possible way to achieving this was proposed by R. Assmann [30, 31]. His idea is to abandon the present passive machine protection and to instead adopt an active protection system, where emergency kickers are distributed along the main linac. Based on information from beam-quality monitors for both main and drive beams, the emergency kickers extract the main-beam bunches onto a dump whenever a problem is detected with either the preceding bunches of the main beam or with one of the two neighboring drive beams. These kickers must always be fired before a full bunch train can impact on the collimators, for which no longer enormous beta functions or dispersion are needed.

The overall layout of the active emergency-dump system is illustrated in Fig. 27 [31]. Emergency dumps are foreseen at the start or end of each drive beam sector (21 per side). The beam quality is monitored in the main linac just upstream of the emergency kicker, in the adjacent drive-beam turn-around loops, and at the end of the last drive-beam decelerator of the preceding drive beam. The beam quality signals travel in beam direction towards the kicker. The solution is economical in that the drive-beam dumps could also be used for disposing the main beam in case of emergency, as is shown in Fig. 27.

To deflect a 1.5-TeV beam at the end of the linac by 1 cm over 50 m, an integrated kick strength of 1 Tm or 300 MV is needed. Primary requirements for the CLIC emergency kicker are summarized in Table 9.

Table 9: Parameters of proposed emergency kicker system for active machine protection in the CLIC main linac.

kick strength	>1 Tm or >300 MV
pulse length	60 ns
repetition rate	up to 150 Hz

Halo Kicker

Another application of interest for collimation would be a 'halo kicker', i.e., a kicker which deflects the beam halo to larger amplitudes without using a low-gap scatterer or primary collimator, in order both to avoid destruction of the latter and to reduce wake fields, which become smaller for larger apertures. A solution proposed by F. Caspers [32] is sketched in Fig. 28. Similar nonlinear pick ups were indeed developed for stacking with stochastic cooling (signal-wise separation of hot low-intense injected and cold intense stacked beams on two different orbits for cooling with two independent systems) at the CERN AA in the 1980s [33] and also proposed for LHC halo cleaning [34]. The figure refers to a horizontal halo kicker with $\sigma_x \gg \sigma_y$. An equivalent vertical halo kicker would have to be positioned at a location with $\beta_y \gg \beta_x$ and $\sigma_y \gg \sigma_x$. Preliminary halo-kicker parameters are listed in Table 10.

Table 10: Parameters of a hypothetical CLIC halo kicker.

current	∼100 A
pulse length	60 ns
repetition rate	up to 150 Hz

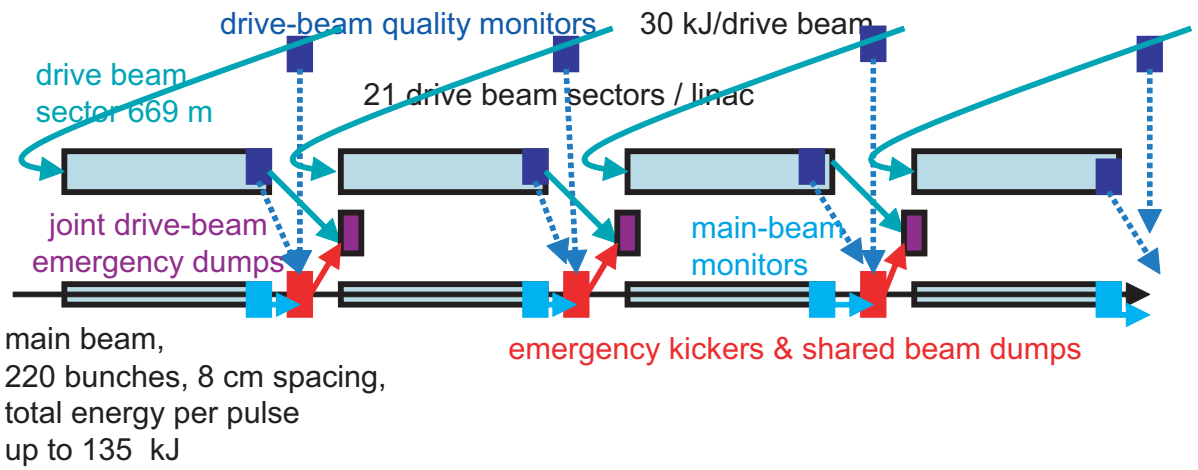

Figure 27: Emergency kickers for active machine protection and shared beam dumps along the CLIC main linac [31].

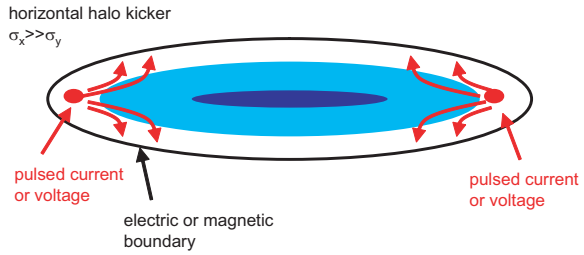

Figure 28: Schematic of a nonlinear horizontal halo kicker [32].

Pulsed Flux Concentrator for Positron Target

Another element requiring a high pulsed field is the flux concentrator behind the positron target. CLIC requirements are summarized in Table 11, assuming that the positrons are produced by a Compton-laser scattering source [35].

Table 11: Parameters of pulsed flux concentrator.

field	> 10 T
pulse length	56 μs
repetition rate	150 Hz

An active development programme for pulsed flux concentrators is ongoing at BINP as part of the R&D for VEPP-5 (and the former NLC) [36]. Figures 29 and 30 show the BINP 1-kJ/pulse 120-Hz modulator, which provides 31 kA current at 4 kV voltage. Figures 31 and 32 present photos of the flux-concentrator magnet itself. Powered by the modulator, it achieves a peak field of 12 T at 50-Hz repetition rate. The measured longitudinal and transverse magnetic fields in this magnet as a function of longitudinal position are displayed in Fig. 33.

Figure 29: BINP modulator for the VEPP-5 positron flux concentrator developed by A.D. Chernikian [36].

Pulsed Wiggler in Main Linac

Wiggler magnets in the main linac could provide additional damping and reduce the emittance below the values extracted from the damping ring. Such use of wigglers was first proposed by Dikansky and Mikhailichenko [37]. A similar scheme was later studied specifically for CLIC [38]. If the transverse normalized emittance is to be reduced from a value ϵ_0 to ϵ_{final}, the optimum beam energy for the additional linac wiggler is given by [38]

$$E_{\rm opt} = \sqrt{\frac{G}{a}}\frac{1}{\hat{B}} \approx 340 \text{ T GeV}\frac{1}{\hat{B}} \,, \qquad (7)$$

where G denotes the accelerating gradient in GeV/m taken to be 150 MV/m, $\hat{B}$ is the peak wiggler field, and

$$a \equiv \frac{2c^2e^2r_e}{3(m_ec^2)^3} \approx 1.3 \times 10^{-6}\,\frac{1}{\text{GeV m T}^2} \,. \qquad (8)$$

Figure 30: BINP modulator for the VEPP-5 positron flux concentrator developed by A.D. Chernikian [36].

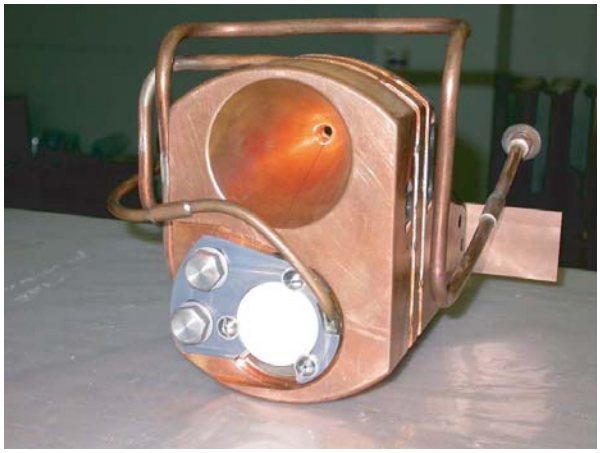

Figure 31: BINP flux-concentrator magnet [36].

For a 10-T peak field, the optimum energy is 34 GeV. This energy is optimum in the sense that the total additional length required is minimized. At the optimum energy, the lengths of the wigglers equal the lengths of the re-accelerating rf sections. The minimum value of the total additional length (the sum of wigglers and re-acceleration)

Figure 32: BINP flux-concentrator magnet [36].

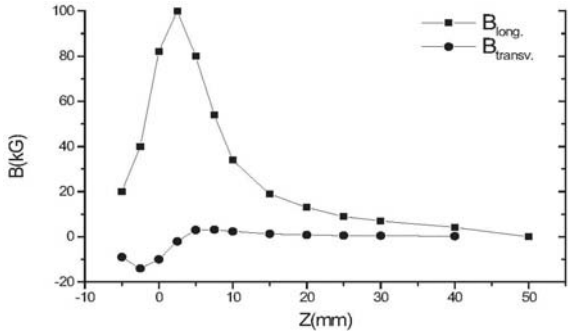

Figure 33: Measured longitudinal and transverse field profile as a function of longitudinal position for the BINP flux concentrator [36]. The positron production target (e.g., liquid metal jet) is located $z = 0$ mm.

is equal to

$$L_{\rm tot} = 4 \ln \left(\frac{\epsilon_0}{\epsilon_f} \right) \frac{1}{\sqrt{aG\hat{B}}} \,. \tag{9}$$

The length is inversely proportional to the peak magnetic field. At a wiggler peak field of 10 T, a length of 5.2 km would be needed in order to damp the beam transversely by a factor 300 [38]. Figure 34 displays the total additional length as a function of beam energy for two different wiggler peak fields. If the transverse emittances should be decreased by a factor of two only, one is still faced with a length of about 600 m for a 10-T field. An further complication is that, for a 10-T field, the emittance growth from quantum excitation becomes significant if the wiggler period exceeds 1.5 cm [38].

A pulsed wiggler might reach a higher field than a static one. Minimal requirements for a pulsed linac wiggler are compiled in Table 12.

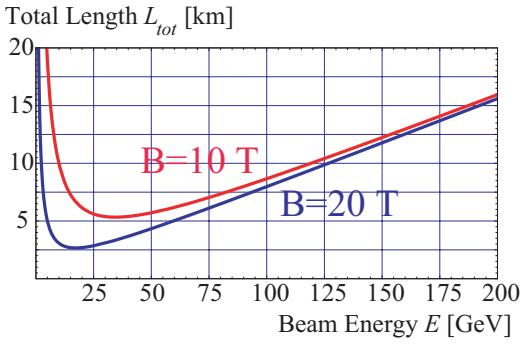

Figure 34: Length of linac damping section as a function of beam energy at wiggler peak fields of 10 and 20 T, for an emittance reduction by a factor of 330 [38].

Table 12: Parameters of pulsed linac wiggler.

field	> 10 T
period	< 1.5 cm
total wiggler length	>100 m
pulse length	60 ns
repetition rate	150 Hz

Long-Range Beam-Beam Compensation

Due to the crossing angle and the short bunch spacing, different CLIC bunches experiences different numbers of long-range collisions before they reach the main collision point. The siutation is sketched in Fig. 35. Transient deflections at the start of a bunch train could be harmful both for the colliding bunches and for the collision products (debris and coherent pairs). For example, without any countermeasure the collision point would shift by $1 - 2\ \sigma_x^*$ during the train passage, due to the increasing number of long-range collisions affecting the incoming bunches.

In order to minimize such transient effects, a pulsed compensator, also called 'wire lens' or 'BBLR', could be used, similar to the one proposed for the LHC [39]. Parameters are listed in Table 13.

Table 13: Parameters of long-range beam-beam compensator.

max. current	27 A
rise time	29 ns
flat top	30 ns
repetition rate	150 Hz

Spent Beam Extraction

The extraction of the spent beam is challenging for a multi-TeV collider, since the energy spread after collision

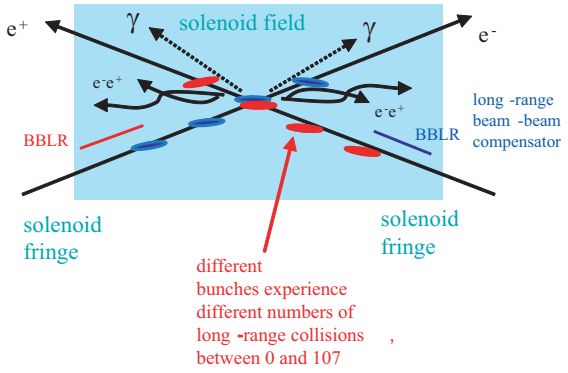

Figure 35: Schematic of the CLIC interaction region with crossing angle, detector solenoid field, multiple bunches, beamstrahlung photons, coherent pairs, and hypothetical long-range beam-beam compensator.

is about 100% (or even 200% counting the coherent pair particles of opposite sign). Figure 36 compares the spent beam energy spectrum at 3 TeV with the one at 500 GeV. Figure 37 shows the energy distribution of the coherent pairs from 3-TeV collisions.

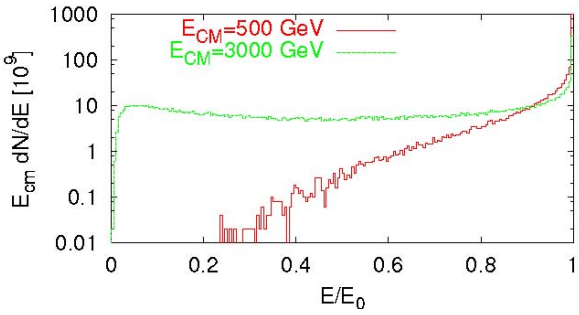

Figure 36: Energy distribution of the spent beam for centre-of-mas energies of 500 GeV and 3 TeV, simulated using the code Guinea-Pig [18, 40].

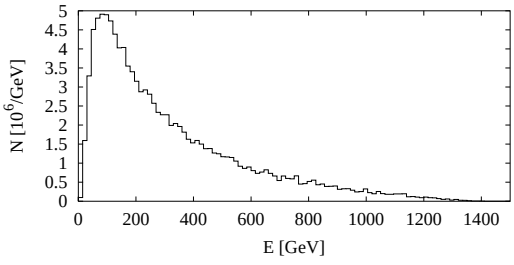

Figure 37: Energy distribution of coherent pairs for a centre-of-mas energy of 3 TeV, simulated using the code Guina-Pig [18].

A first exit-line layout for CLIC was proposed in

Ref. [40]. This line contains no quadrupoles in view of the enormous energy spread of the beam to be transported. It is reproduced in Fig. 38. A challenging question for RPIA2006 and beyond is whether we can use pulsed switching devices to either confine the low-energy particles or to reduce the energy spread of the spent beam. The latter could be achieved with an induction rf system, whose accelerating field depends on the horizontal position. Unfortunately, for such a compensation to be meaningful extremely large induction voltages or fields would be required in case of a high-energy 3-TeV collider. The requirements on the pulsed extraction element are summarized in Table 14.

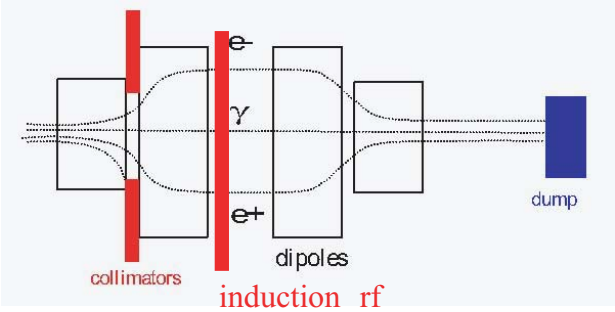

Figure 38: Schematic layout of a draft CLIC exit line which separates charged and neutral debris components using a chicane prior to disposal on a beam dump [40].

Table 14: Parameters of induction device in extraction line.

integrated field	$>$100 Tm, $>$ 30 GV
pulse length	60 ns
pulses per second	150

SUMMARY

CLIC is a future electron-positron linear collider with high accelerating gradient using a drive beam as rf source.

New pulsed-power technologies may offer solutions for its combiner-ring extraction kickers and solid-state induction drive-beam modulators. The same technologies could furnish economical implementations of the fast IP feedback and, less likely, the crab cavities. Finally, advanced technologies might further boost the CLIC performance by providing emergency kickers and beam dumps, halo kickers, pulsers for positron flux concentrator or beam-beam compensation, damping-ring rf, tools for spent-beam handling, or pulsed linac wigglers.

ACKNOWLEDGEMENTS

We thank Ken Takayama and the Tokyo Institute of Technology for their interest and support.

REFERENCES

[1] CLIC Physics Study Group, "Physics at the CLIC Multi-TeV Linear Collider," edited by M. Battaglia, A. de Roeck, J. Ellis, and D. Schulte, CERN-2004-005 (2004).

[2] International Linear Collider Technical Review Committee, "ILC-TRC," G. Loew et al, web site *http://www.slac.stanford.edu/xorg/ilc-trc/2002/* (2002).

[3] H. Braun, "CLIC", 8th ICFA Seminar on "Future Perspectives in High Energy Physics," Daegu, Korea, 28 September – 1 October 2005, web site *http://chep.knu.ac.kr/ICFA-Seminar/* (2005).

[4] A. Sessler, "The Free Electron Laser as a Power Source for a High-Gradient Accelerating Structure," in Laser Acceleration of Particles (P. Channel, ed.), AIP 91, American Institute of Physics, p. 154 (1982).

[5] W. Schnell, "A Two-Stage Linear Collider Using a Superconducting Drive Linac," CLIC Note 13 (1986).

[6] C. Achard et al., "A Demonstration of High-Gradient Acceleration," CERN-AB-2003-048, CLIC Note 569 (2003).

[7] A. Grudiev, W. Wünsch, "A Newly Designed and Optimized CLIC Main Linac Accelerating Structure," LINAC 2004, Lübeck (2004).

[8] H. Braun, "CLIC," at 8th ICFA Seminar on 'Future Perspectives in High Energy Physics,' Daegu, Korea (2005).

[9] R. Corsini, "R&D on Multi-TeV Collider — Status and Perspectives," HEP-EPS 2005 Conference Lisbon (2005).

[10] R. Brinkmann et al (Eds.), "TESLA Technical Design Report," DESY 2001-011 (2001).

[11] SCRF Linac Proton Driver Study Group, G.W. Foster (Ed.), "An 8-GeV Superconducting Linac Proton Driver," FNAL Draft TM Note (2006).

[12] R.L. Cassel et al., "The Prototype Solid State Induction Modulator for SLAC NLC," PAC 2001 Chicago (2001).

[13] R. Assmann et al, "A 3-TeV e+e- Linear Collider based on CLIC Technology," CERN 2000-008 (2000).

[14] P. Burrows, "Overview of the Very Fast Intra-Train Beam Feedback Work (FONT)," CLIC BDS Day 22.11.2005 (2005)

[15] P.N. Burrows et al, "Tests of the FONT3 Linear Collider Intra-Train Beam Feedback System at the ATF," PAC2005 Knoxville (2005).

[16] P.N. Burrows, "Optimizing the Linear Collider Luminosity: Feedback on Nanosecond Time Scales," Snowmass 2001 (2001).

[17] D. Schulte, F. Zimmermann, "The Crossing Angle in CLIC," PAC2001 Chicago (2001).

[18] D. Schulte, "High-Energy Beam-Beam Effects in CLIC," PAC'99 New York (1999).

[19] R.B. Palmer, "Energy Scaling, Crab Crossing, and the Pair Problem," Snowmass 1988 (1988).

[20] E. Vogel, private communication (2005).

[21] W. Chou, discussion at RPIA2006 workshop (2006).

[22] J. Jowett, T. Risselada, F. Zimmermann, H. Owen, "Damping Rings for CLIC," PAC2001 Chicago (2001).

[23] M. Korostelev, F. Zimmermann, "Optimization of CLIC Damping Ring Design Parameters," EPAC'02 Vienna (2002).

[24] M. Korostelev, PhD Thesis, U. Lausanne, to be published (2006).

[25] F. Ruggiero, G. Rumolo, F. Zimmermann, Y. Papaphilippou, "Beam Dynamics Studies for Uniform (Hollow) Bunches or Super-Bunches in the LHC: Beam-Beam Effects, Electron Cloud, Longitudinal Dynamics, and Intrabeam Scattering," Proc. RPIA'2002, K. Takayama (ed.), KEK Proceedings 2002-30 (2002)

[26] F. Wang et al, "Coherent THz Synchrotron Radiation from a Storage Ring with High-Frequency RF System," Phys. Rev. Lett. 96, 064801 (2006).

[27] S. Fartoukh, J.B. Jeanneret, J. Pancin, "Heat Deposition by Transient Beam Passage in Spoilers," CLIC-NOTE-477 (2001).

[28] R. Assmann et al., "Collimation for CLIC," HALO'03 Montauk, CLIC-NOTE-579 (2003)

[29] D. Schulte, F. Zimmermann, "Failure Modes in CLIC," PAC'2001 Chicago (2001).

[30] R. Assmann, private communication (2006).

[31] R. Assmann, F. Zimmermann, "Efficient Collimation and Machine Protection for the Compact Linear Collider," EPAC'06 (2006).

[32] F. Caspers, private communication (2006).

[33] F. Caspers, D. Möhl, "Stacking with Stochastic Cooling," Int'l Workshop on Beam Cooling and Related Topics, COOL03, Lake Yamanaka, 19–23 May 2003, and CERN-AB-2004-028 RF (2003).

[34] F. Caspers, "Techniques of Stochastic Cooling," Workshop on Beam Cooling and Related Topics, 14–18 May 2001, Bad Honnef CERN/PS 2001-17 (RF) (2001).

[35] F. Zimmermann et al, "CLIC Polarized Positron Source Based on Laser-Compton Scattering," EPAC'06 (2006).

[36] P. Logachev, "R&D on the NLC Positron Production System in BINP," 6th Workshop on Higher Luminosity B Factory, KEK, November 16–18, 2004 (2004).

[37] N.S. Dikansky, A.A. Mikhailichenko, "Straightline Cooling System for Obtaining Beams of Electrons and Positrons with Minimal Emittance," EPAC'92 Berlin (1992).

[38] H. Braun, M. Korostelev, F. Zimmermann, "Potential of Non-Standard Emittance Damping Schemes for Linear Colliders," APAC'04 Gyeongju, Korea (2004).

[39] J.-P. Koutchouk, "Correction of the Long-Range Beam-Beam Effect in LHC Using Electromagnetic Lenses," PAC 2001, Chicago (2001).

[40] M. Aleksa et al, "CLIC Beam Delivery System," Nanobeam'02 Lausanne (2002).